Design, Synthesis, and Estrogenic Activity of a Novel Estrogen Receptor Modulator—A Hybrid Structure of 17β-Estradiol and Vitamin E in Hippocampal Neurons

Liqin Zhao,[†] Chunyang Jin,[‡] Zisu Mao,[†] Madathil B. Gopinathan,[‡] Kenneth Rehder,*[,‡] and Roberta D. Brinton*[,†]

Department of Pharmacology and Pharmaceutical Sciences, School of Pharmacy, University of Southern California, Los Angeles, California 90089, and Center for Organic and Medicinal Chemistry, RTI International, Research Triangle Park, North Carolina 27709

Received May 9, 2007

We recently discovered that ICI 182,780 (**1**), an antagonist of estrogen receptor (ER)-dependent proliferation in reproductive tissues, functions as an estrogenic agonist in primary neurons. The present study investigated whether the agonist properties of **1** in neurons could be translated into structural analogs. 7α-[(4*R*,8*R*)-4,8,-12-trimethyltridecyl]estra-1,3,5-trien-3,17β-diol (**2**), a hybrid structure of 17β-estradiol and vitamin E, was synthesized and found to bind to both ERα and ERβ. *In vitro* analyses demonstrated that **2** was neuroprotective and effective in activating molecular mechanisms associated with estrogenic agonist activity in rat primary hippocampal neurons. Collectively, the data support an estrogenic agonist profile of **2** action comparable to **1** in primary neurons, confirming that estrogenic activity of **1** in neurons is not a unique phenomenon. These results provide support for the development of a brain-selective ER modulator, with potential as an efficacious and safe estrogen alternative to prevent Alzheimer's disease and cognitive decline in postmenopausal women.

Introduction

Alzheimer's disease (AD[a]), a devastating neurodegenerative condition associated with impaired memory and cognitive function, affects an estimated 4.5 million people in the United States.[1] Of those affected with AD, 68% are female and 32% are male.[2−4] The greater female vulnerability to AD has been associated with the marked decrease in the level of estrogen circulating in postmenopausal women.[5,6] In addition to its multifaceted health-promoting effects on a woman's body, such as counteraction of postmenopausal symptoms and preservation of bone density, research over the past two decades has supported the use of estrogen therapy (ET) for the prevention of AD and other age-related neurodegenerative insults when timely initiated[7−9] based on the "healthy cell bias" of estrogen actions in neurons.[10−12] However, side effects of the currently available ET, such as neoplasm[13] and thrombogenesis,[14,15] remain serious risks to patients. Therefore, there is an unmet medical need for estrogen alternatives that are free of long-term side effects and are perceived as safe by physicians and patients.

In previous studies, we examined whether existing clinically relevant selective estrogen receptor modulators (SERMs) would exert estrogenic agonist effects comparable to the endogenous estrogen 17β-estradiol in the brain. Using neuronal responsive predictors associated with estrogen actions in neurons as target outcomes, we unexpectedly discovered that the full antagonist to the nuclear estrogen receptor (ER), ICI 182,780 (**1**), acted as a full estrogenic agonist in primary neurons at clinically relevant concentrations.[16]

Compound **1** is a 7α-alkylsulfinyl analog of 17β-estradiol and binds to both ERα and ERβ with an affinity comparable to 17β-estradiol.[17] By competing for the ER ligand binding site and subsequently driving the receptor to reorient into a characteristic antagonistic conformation,[18] **1** abolishes the nuclear ER-dependent proliferative actions of estrogen in reproductive organs such as the breast and uterus.[19] In addition, **1** is devoid of estrogen-like agonist activity in these organs, in contrast to the partial estrogen agonist/antagonist tamoxifen (TMX), and TMX-resistant tumors are sensitive to **1** treatment.[19] As a result, the FDA has approved the use of **1** as an adjuvant endocrine therapy to treat ER-positive metastatic breast cancers in postmenopausal women with disease progression following first-line antiestrogen therapy (i.e., for TMX-resistant breast cancers).[20] Therefore, from a therapeutic development perspective, our finding that **1** acts as an estrogenic agonist in neurons provides a promising translational opportunity for the development of a brain-selective SERM mimicking the beneficial effects of an estrogen agonist in the brain, while lacking or antagonizing activation of estrogenic proliferative responses in reproductive organs.[10]

Our initial efforts to develop a brain-selective SERM have two objectives: design and synthesize structural analogs of **1** to (a) replicate the promising in vitro activity of **1**[16] and (b) cross the blood−brain barrier (BBB) because **1** does not.[19] Herein, we report our efforts to design and synthesize the first candidate compound, 7α-[(4*R*,8*R*)-4,8,12-trimethyltridecyl]estra-1,3,5-trien-3,17β-diol (**2**), and first-stage analyses of its estrogenic activity in cell-based assays in primary hippocampal neurons.

Results and Discussions

Computer Modeling and Design. Using computer-aided molecular modeling approaches, we first analyzed the three-dimensional (3D) structural features of **1** in complex with ER. Analyses demonstrated that, in comparison with the ER full agonist 17β-estradiol, the nuclear ER full antagonist **1** has two structural domains that carry out distinct functions. First, the

* To whom correspondence should be addressed. Tel.: 323-4421430, Fax: 323-2247473, E-mail: rbrinton@usc.edu (R.D.B.); Tel.: 919-5416681, Fax: 919-5416499, E-mail: krehder@rti.org (K.R.).

[†] University of Southern California.

[‡] RTI International.

[a] Abbreviations: AD, Alzheimer's disease; ET, estrogen therapy; ER, estrogen receptor; SERM, selective estrogen receptor modulator; TMX, tamoxifen; RAL, raloxifene; AF, activation function; BBB, blood−brain barrier; DIV, days in vitro; ERK, extracellular signal-regulated kinase; Akt, protein kinase B; PDB, Protein Data Bank.

10.1021/jm070546x CCC: $37.00
Published on Web 08/14/2007

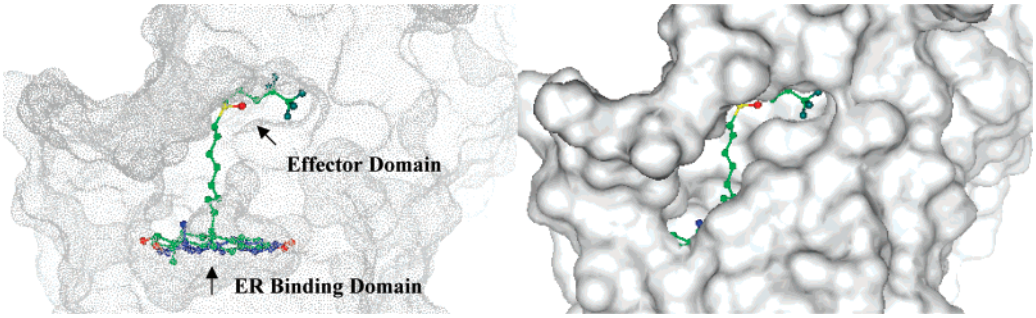

Figure 1. 3D-bound confirmations of 17β-estradiol and **1** in human ERα (hERα). The complex model of 17β-estradiol/hERα was generated based on the crystallographic structural coordinates downloaded from the Protein Data Bank (PDB ID: 1ERE). The complex model of **1**/hERα was generated from docking calculations with GOLD, followed by energy optimization with InsightII/Discovery. The complex models of 17β-estradiol/hERα and **1**/hERα were superimposed by aligning the 3D coordinates of hERα. Both 17β-estradiol and **1** are depicted in "ball and stick" format and colored based on the atom types designated in InsightII: red, oxygen atoms; yellow, sulfur atoms; aqua, fluorine atoms; for distinction, the carbon atoms in 17β-estradiol and **1** are colored in blue and green, respectively. hERα is rendered by its solvent accessible surface depicted in dots or solid format. These models revealed that the "head moiety", also referred to as the "ER binding domain" in **1**, the 17β-estradiol core structure, lies in the center of the ligand binding pocket on hERα, in a similar mode to that of 17β-estradiol, although the 13β-methyl groups in both structures are situated in opposite orientations. The "tail moiety" (7α-alkylsulfinyl side chain), also referred to as the "effector domain" in **1**, protrudes out of the ligand binding pocket and nestles in a relatively hydrophobic groove. This is proposed to be the driving force for the remodeling of helix 12, leading to impaired ER dimerization and the resultant blockage of nuclear uptake. Images were generated with InsightII 2000 on a SGI Octane graphical workstation equipped with the IRIX 6.5 operating system.

"head moiety", represented by the 17β-estradiol core structure, is accommodated into the ligand binding pocket on ER in a similar mode to that of 17β-estradiol, although the 13β-methyl groups on both structures are situated in opposite orientations (Figure 1). Owing to its driving role in the ligand binding to ER, as revealed in our previous analyses,[10,21] we refer to this structural moiety as the "ER binding domain" in **1**. Second is the "tail moiety", represented by the bulky side chain substituted on the 7α position of 17β-estradiol core structure, which protrudes out of the ligand binding pocket and occupies the same channel on ER as occurs with ICI 164,384 (**3**), a structural analog of **1** (Figure 1).[18] In comparison with many ER partial agonists/antagonists, such as TMX and raloxifene (RAL) with relatively shorter "tail moieties" attached to their ER binding core structures,[10] it has been suggested that the extended terminal portion of the "tail moiety" in **1** nestles within the activation function-2 (AF-2) cleft that precludes helix 12, a structural component on ER that is crucial for ER dimerization, from staying in the same cleft.[22] This indicates a unique reorientation distinct from either its characteristic agonist orientation, as seen with 17β-estradiol, in which helix 12 is aligned over the ligand binding pocket,[22] or its partial antagonist orientation, as seen with TMX or RAL, in which helix 12 orients along the coactivator binding surface in AF-2.[22] As a result, such a reorientation of helix 12 induced by **1** leads to a full abolition of ER transcription regulated by both AF-1 and AF-2, which accounts for its "pure" antiestrogenic effect, particularly in reproductive tissues.[17,19] In addition, it has been suggested that this displacement of helix 12 impairs ER dimerization and inhibits the translocation of ER into the nucleus.[23] In view of the significant role of the "tail moiety" in **1** in shifting the direction of its impact on the nuclear ER function, we refer to this structural moiety as its "effector domain". Overall, these comparative analyses provide important insights into the rational design of novel ICI mimics that are anticipated to induce a pharmacological profile consistent with **1**, that is, estrogenic agonist activity in the brain, while lacking or antagonizing estrogenic proliferative action in reproductive tissues.

Guided by insights derived from the above analyses, we proposed a number of novel ICI analogs predicted to possess improved brain penetration compared to **1**. These analogs have structural moieties associated with endogenously occurring

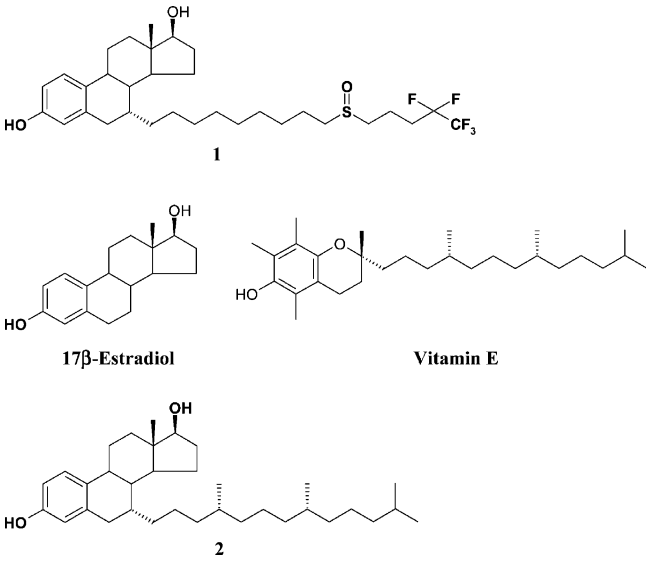

Figure 2. Compound **2** is a hybrid structure of 17β-estradiol and vitamin E.

compounds, suggesting the toxicity of the analogs may be less problematic. One representative compound, **2**, is a hybrid structure of 17β-estradiol and vitamin E (Figure 2), both of which are brain permeable and widely used in humans.[24] While a structure composed of two BBB-penetrable moieties, estrogenic "head moiety" and vitamin-like "tail moiety", cannot be guaranteed to cross the BBB, it would presumably have greater potential than combinations composed of brain-inaccessible moieties. In addition, replacement of the "tail moiety" in **1** (cLogP of 8), with a vitamin E-like hydrophobic side chain, increases the overall lipid solubility of **2** (cLogP of 12), comparable to that of vitamin E (clogP of 11). While this lipophilicity falls out of the range defined by the "Lipinski rule of five" for druggability and brain penetration,[25] vitamin E has a similar high lipophilicity, yet, can readily enter the brain.[24] In view of the complexity of the biological features of BBB[26] and the multiple factors that contribute to BBB penetration,[27,28] by deliberately mimicking the physicochemical properties of vitamin E that may jointly impact its brain entry, including lipophilicity, molecular shape and associated conformational

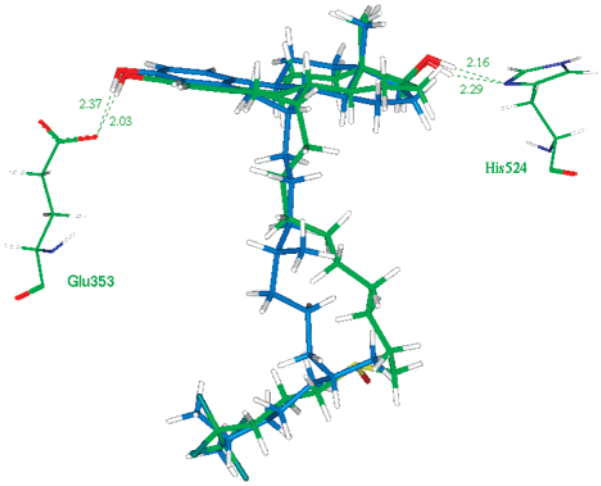

Figure 3. 3D-bound conformations of **1** and **2** in hERα. Models were derived from docking calculations with GOLD. Both **1** and **2** are depicted in "stick" format and colored based on the atom types designated in InsightII: red, oxygen atoms; yellow, sulfur atoms; aqua, fluorine atoms; except that for distinction, the carbon atoms in **1** and **2** are colored in green and sky blue, respectively. Residues, Glu353 and His524 on hERα, which form hydrogen bond interactions with both ligands depicted in dashed green lines, are shown in "stick" format and colored based on the atom types. These models revealed that **2** binds to hERα in a mode similar to **1**, suggesting the functional similarity between two compounds. Image was generated with InsightII 2000 on a SGI Octane graphical workstation equipped with the IRIX 6.5 operating system.

flexibility, and specifically, distribution of a hydrophilic ("head")/hydrophobic ("tail") structural balance that may impact the interaction with the BBB membrane−water complex, as revealed by recent membrane-interaction quantitative structure−activity relationship (MI-QSAR) models,[29,30] **2** is anticipated to have a similar BBB penetrative ability to vitamin E. Moreover, **2** has a smaller molecular mass of 496 than **1** at 552 and, therefore, falls below the suggested threshold of 500 for a brain-permeable molecule.[31,32] Most importantly, as revealed in Figure 3, GOLD docking analyses indicated that **2** binds to hERα in an energy-favorable fashion, similar to **1**. In addition, hydrogen bond interactions were observed in both compounds between 3, 17β-OH groups, and the residues, glu353 and His524, respectively, along the ligand binding site in hERα. The similar binding modes and ligand−receptor intermolecular interactions exhibited by **1** and **2** suggested that **2** would exert a tissue-selective modulation of ER that is consistent with **1**.

Chemistry. Synthesis of 7α-substituted estradiol derivatives has been generally achieved by copper-promoted nucleophilic 1,6-conjugate addition of Grignard reagents to steroidal dienones such as 6-dehydrotestosterone 17-acetate.[33,34] However, such additions usually lead to a mixture of 7α- and 7β-epimers and, subsequently, require rearomatization to generate the aromatic A-ring. More recently, another synthetic approach using alkyl iodides to alkylate 3,17-diprotected 6-ketoestradiols was found to be more efficient and versatile for synthesis of 7-substituted estradiols with high stereoselectivity.[35−40] Accordingly, our synthesis of 7α-[(4*R*,8*R*)-4,8,12-trimethyltridecyl]estra-1,3,5-trien-3,17β-diol (**2**) was accomplished following the second synthetic strategy, starting from preparation of the side chain intermediate, (4*R*,8*R*)-1-iodo-4,8,12-trimethyltridecane (**8**; Scheme 1). Ozonolysis[41] of phytol (**4**) with ozone at −78 °C followed by a reductive workup gave phytone (**5**) in 76% yield. Baeyer−Villiger oxidation of **5** was first attempted using 5 equiv of 3-chloroperbenzoic acid (*m*-CPBA) in refluxing chloroform to afford **6** in 54% yield. However, the product contained trace impurities, which could not be removed by chromatographic purification. Further reaction optimization was successfully achieved through the use of bis(trimethylsilyl)peroxide and tin tetrachloride catalysis,[42] and (4*R*,8*R*)-1-acetoxy-4,8,12-trimethyltridcane (**6**) was obtained in 62% yield. Hydrolysis of **6** proceeded quantitatively with *p*-toluenesulfonic acid in refluxing methanol to yield **7**, which was converted to (4*R*,8*R*)-1-iodo-4,8,12-trimethyltridecane (**8**) in 85% yield upon treatment with iodine, triphenylphosphine, and imidazole.

With the side chain precursor **8** achieved, focus was next directed toward the synthesis of a suitably protected steroid core and subsequent alkylation with **8** (Scheme 2). Oxidation of 3,-17β-estradiol diacetate (**9**) with chromium trioxide and 3,5-dimethylpyrazole gave ketone **10** in 44% yield.[43] Hydrolysis of **10** with potassium hydroxide afforded 6-oxo-3,17β-estradiol (**11**), quantitatively. Crude **11**, used without further purification, was then reprotected with tetrahydropyranoxy (THP) groups by reaction with dihydropyran (DHP) to provide **12** in 98% yield.[44] The critical alkylation on the C7-position of the steroid was achieved by treatment of the potassium enoxyborate of **12**,[37] generated using potassium *t*-butoxide and triethylborane, with (4*R*,8*R*)-1-iodo-4,8,12-trimethyltridecane (**8**) in dimethoxyethane (DME). The 7α-substituted steroid **13** was obtained as a single diastereomer in 34% yield. To our knowledge, this is one of the highest yields reported for the alkylation with this size alkyl substituent. Finally, deprotection of the THP groups and deoxygenation of the 6-keto functionality were simultaneously accomplished with boron trifluoride etherate and triethylsilane[37] to produce **2** in 83% yield.

The α-configuration for the C7-substituent of **2** was assigned based on two-dimensional NMR (COSY and ROESY) spectral analyses. Strong correlation was observed between H(7) and H(8), indicating that these two protons were proximal (Figure 4). Based on the known β-stereochemistry of H(8), the H(7) is also assigned the β position. No correlation between H(7) and H(9) was detected. The C6-benzylic protons were clearly evident at δ 2.86 and 2.72, with coupling constants of 4.8, 16.9, and 16.9 Hz, respectively, which is also consistent with the structure.

Estrogenic Activity of 2. We first determined the binding affinity and specificity of **2** to ERα and ERβ. A fluorescent polarization competitive binding assay was used, which is composed of purified baculovirus-expressed human ERα or ERβ and a fluorescent estrogen ligand EL Red. Progesterone was used as a negative control, and known ER ligands, 17β-estradiol, **1**, and genistein, were used as positive controls. The ability of the test compounds at serially diluted concentrations (100 pM to 10 μM) to compete with the estrogen ligand EL Red for binding to ERα or ERβ was assessed by a change in polarization values at 535 nm/590 nm excitation/emission. Figure 5 shows the competition binding curves of the test compounds for both ERα and ERβ. As expected, the negative control compound, progesterone, does not bind to either ER. The IC_{50} determined from the binding curves for positive estrogen controls, 17β-estradiol (4.7 and 16.7 nM for ERα and ERβ, respectively) and **1** (4.9 and 44.1 nM for ERα and ERβ, respectively), are consistent with the previously reported values.[21] Moreover, the assay was sufficiently sensitive to differentiate the ERβ-binding preference of the phytoestrogen, genistein, with a 46.8-fold binding selectivity over ERα, which is consistent with results derived from alternative methods such as the radioligand assay.[45] These comparative analyses demonstrate the reliability of this assay in determining the binding profiles of small compounds to both ERs. Compound **2** comparably bound to both ERα, with a binding IC_{50} of 193 nM, and ERβ, with a binding IC_{50} of 267

Scheme 1[a]

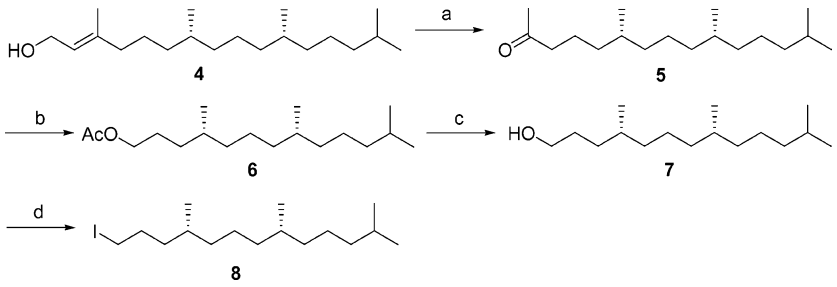

[a] Reagents and conditions: (a) ozone, MeOH−CH_2Cl_2, −78 °C, then $(CH_3)_2S$, room temperature, 2.5 h, 76%; (b) $SnCl_4$, $(TMSO)_2$, CH_2Cl_2, room temperature, 4 h, 62%; (c) TsOH, MeOH, reflux, 6 h, 100%; (d) Ph_3P, imidazole, I_2, CH_2Cl_2, room temperature, 2 h, 85%.

Scheme 2[a]

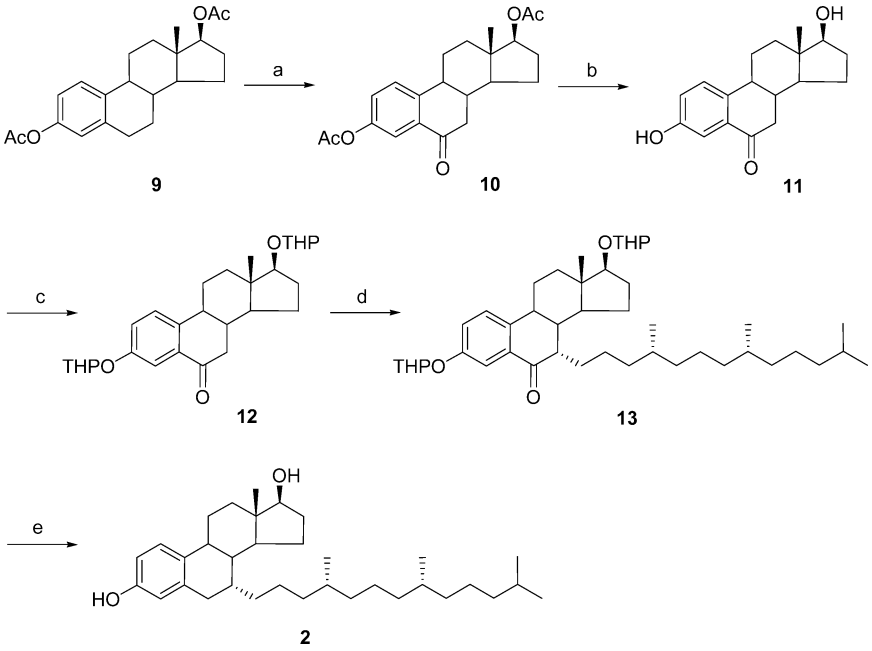

[a] Reagents and conditions: (a) CrO_3, 3,5-dimethylpyrazole, −20 °C, 5 h, 44%; (b) KOH, MeOH−H_2O, room temperature, 4 h, 100%; (c) dihydropyran, PPTS, CH_2Cl_2, reflux, 3 h, 98%; (d) KO*t*-Bu, Et_3B, DME, room temperature, 1 h, then **8**, overnight, 34%; (e) Et_3SiH, BF_3·Et_2O, CH_2Cl_2, room temperature, overnight, 83%.

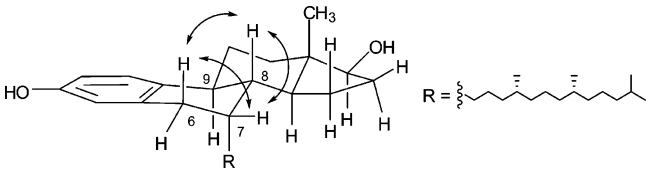

Figure 4. Key ROESY correlations of **2**.

nM. Although the binding affinity of **2** to both ERs is approximately 10- to 50-fold lower than those for 17β-estradiol and **1**, they are well within the therapeutic development range.

To determine whether **2** would act as an estrogenic agonist in neurons comparable to 17β-estradiol and **1**, we first evaluated the activity of **2** to protect neurons against the neurodegenerative insult, a supraphysiological concentration of glutamate-induced neurotoxicity in cultured rat primary hippocampal neurons. Neuronal viability was assessed by dual measurements of lactate dehydrogenase (LDH) release in the culture medium, which served as an indicator of neuronal membrane integrity, and calcein acetoxymethyl ester (AM) staining, which served as an indicator of neuronal metabolic viability. Data shown in Figure 6 demonstrated that **2** promoted neuronal survival in a concentration-dependent manner. The amount of LDH released in the culture medium induced by 200 μM glutamate was significantly reduced by **2** at all test concentrations (1−1000 nM), while the

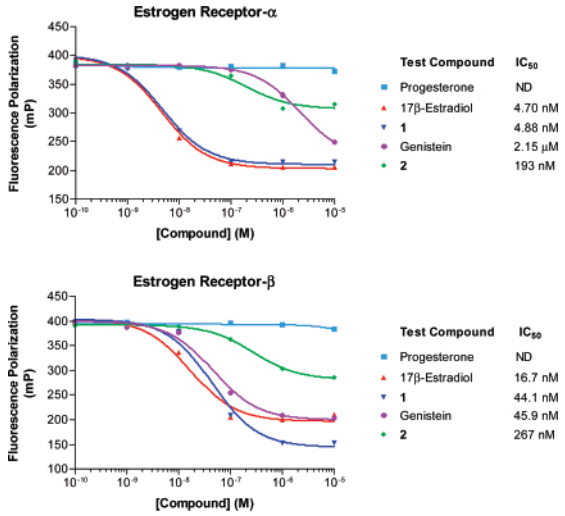

Figure 5. Compound **2** binds to both ERα and ERβ, with comparable IC_{50} values, 192 nM for ERα and 267 nM for ERβ.

efficacy induced by 100−1000 nM was significantly greater than that induced by 1−10 nM of **2** ($^{++}P < 0.01$). There were no significant differences in LDH release between cultures treated with 1 nM and 10 nM (Figure 6A, 38.6 ± 3.8% and

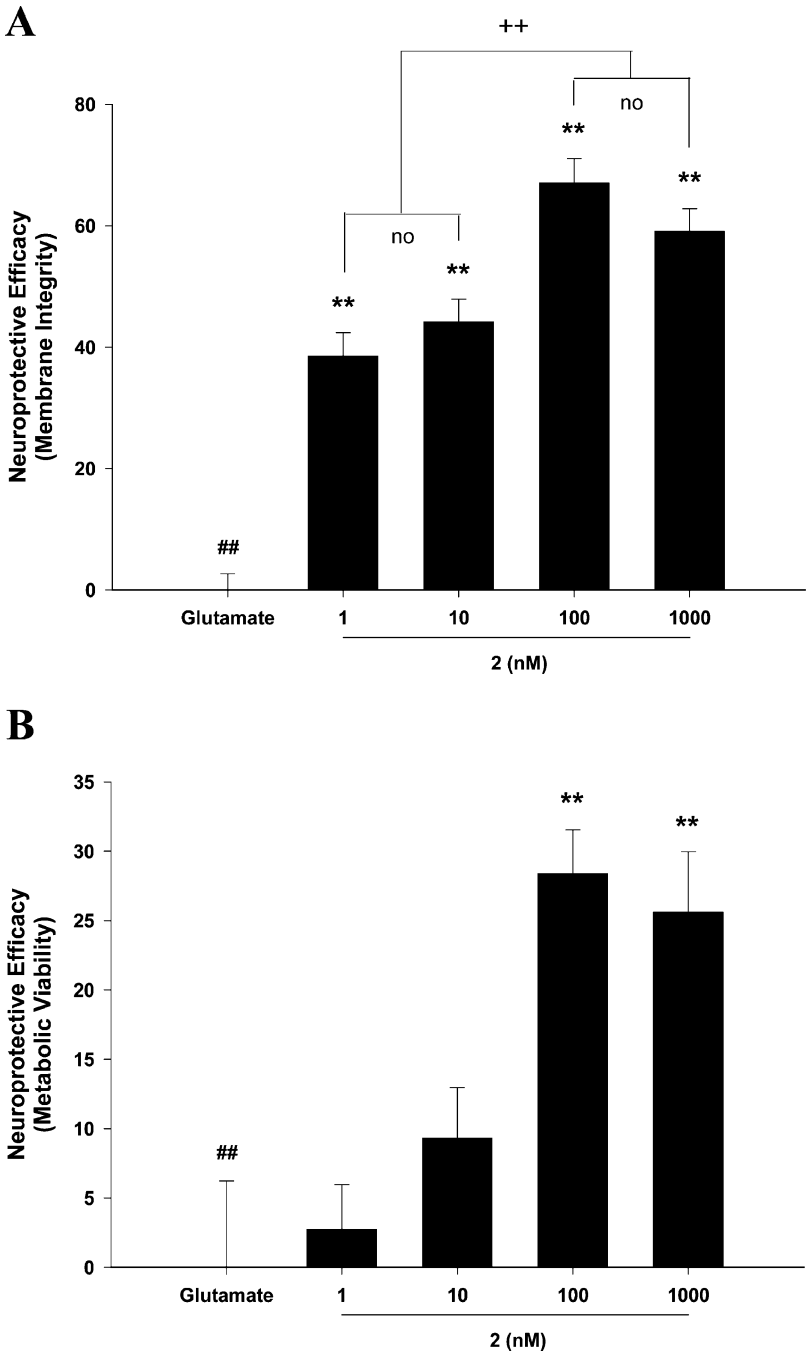

Figure 6. Compound **2** promoted neuronal survival against supraphysiological glutamate-induced neurotoxicity in a concentration-dependent manner in rat primary hippocampal neurons. Neurons grown for 7 DIV were pretreated with vehicle alone or **2** at serially diluted concentrations (1, 10, 100, and 1000 nM) for 48 h prior to exposure to 200 μM glutamate for 5 min, followed by a 24 h recovery. Neuroprotective activity was determined by (A) LDH release in the culture medium, an indicator of neuronal membrane integrity, and (B) calcein AM staining of the live neurons in the culture, an indicator of neuronal metabolic viability, from the same population of neurons. Results are presented as neuroprotective efficacy (NE), which is defined as the percentage of glutamate-induced neurotoxicity prevented by **2** treatment and quantitated by the equation: $NE = (V_2 - V_{glutamate})/(V_{control} - V_{glutamate}) \times 100\%$, where V_2 = the individual value from **2**-treated cultures, $V_{glutamate}$ = the mean value from glutamate alone-treated cultures, and $V_{control}$ = the mean value from vehicle alone-treated control cultures. Data, expressed as mean ± SEM, $n \geq 6$, are derived from a single experiment and are representative of three separate experiments. $^{\#\#}P < 0.01$ compared to vehicle alone treated control cultures, $^{**}P < 0.01$ compared to glutamate alone-treated cultures. $^{++}P < 0.01$ indicates the differences between 1−10 nM and 100−1000 nM of **2** treatment groups.

44.1 ± 3.8% increase in neuronal membrane integrity compared with glutamate alone-treated cultures, respectively, $^{**}P < 0.01$), and between cultures treated with 100 nM and 1000 nM of **2** (Figure 6A, 67.0 ± 4.0% and 59.1 ± 3.7% increase in neuronal membrane integrity compared with glutamate alone-treated cultures, respectively, $^{**}P < 0.01$). Data shown in Figure 6B, derived from calcein AM staining of metabolically live neurons in the cultures, revealed a similar trend in neuronal response to serially diluted concentrations of **2**. A significant increase in neuronal viability was observed in cultures treated with 100−1000 nM of **2** (Figure 6B, 28.4 ± 3.2% and 25.6 ± 4.4% increase in neuronal metabolic viability compared with glutamate alone-treated cultures, respectively, $^{**}P < 0.01$). In contrast, **2** at 1−10 nM was insufficient to prevent the loss of neuronal metabolic activity induced by glutamate insult (Figure 6B, 2.7 ± 3.2% and 9.3 ± 3.7% increase in neuronal metabolic viability compared with glutamate alone-treated cultures, respectively), although 1−10 nM was effective in protecting neurons against

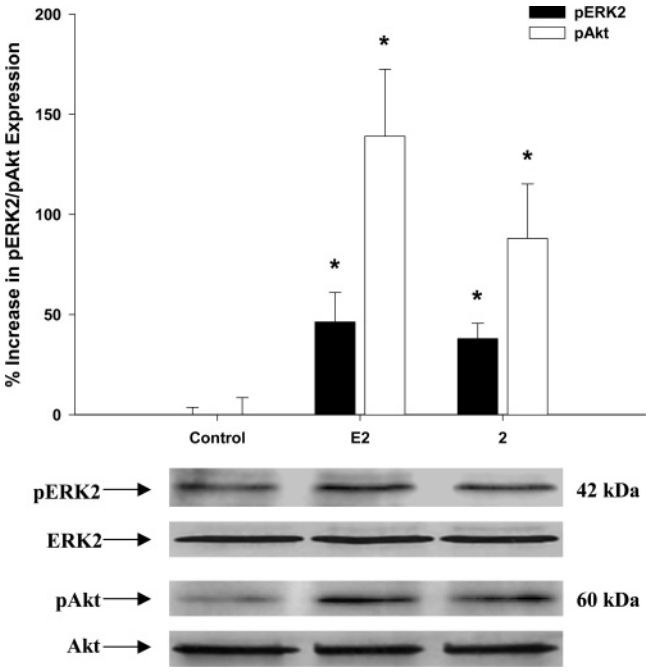

Figure 7. Compound **2** rapidly increased ERK2 and Akt phosphorylation in rat primary hippocampal neurons. Neurons grown for 7 DIV were treated with vehicle alone, E2 (10 nM) or **2** (100 nM) for 30 min followed by Western immunoblotting analyses on phosphorylated and total ERK2 and Akt expression in the whole cell lysate preparation of neurons. pERK2 and pAkt levels were normalized against the levels of total ERK2 and Akt, respectively. Results are presented as percent increase in pERK2 and pAkt expression compared to vehicle alone-treated control cultures and expressed as mean ± SEM, $n = 4$, $^*P < 0.05$. E2: 17β-estradiol.

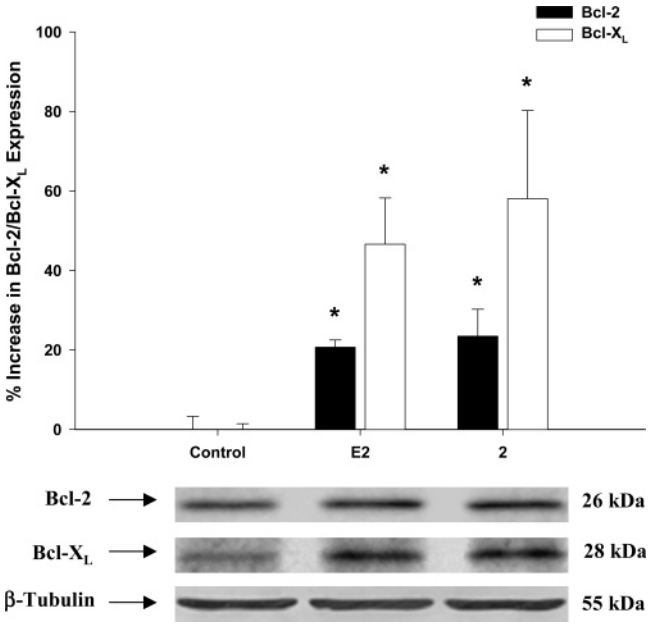

Figure 8. Compound **2** upregulated the anti-apoptotic proteins Bcl-2 and Bcl-X_L expression in rat primary hippocampal neurons. Neurons grown for 7 DIV were treated with vehicle alone, E2 (10 nM), or **2** (100 nM) for 48 h followed by Western immunoblotting analyses on Bcl-2 and Bcl-X_L expression in the whole cell lysate preparation of neurons. β-Tubulin was used as an internal loading control protein. Results are presented as percent increase in Bcl-2 and Bcl-X_L expression compared to vehicle alone treated control cultures and expressed as mean ± SEM, $n \geq 3$, $^*P < 0.05$. E2: 17β-estradiol.

glutamate-induced neuronal membrane damage. These differences in outcomes derived from measurements of different biochemical indicators from the same population of neurons suggested that neuronal membrane damage may be more easily protected and repaired than damage to neuronal metabolic function or it may be due to interassay sensitivity. Results of these analyses are consistent with our previous reports for multiple estrogens and **1**.[16,46] Moreover, a 10-fold less potency associated with **2** than 17β-estradiol and **1**, which exhibited the maximal neuroprotection at 10 nM,[16] is consistent with the differences between the ER binding affinity of **2** and 17β-estradiol and **1**, suggesting that estrogen-inducible neuroprotective activity is associated with ER-mediated signaling cascades. As **2** exhibited a full and optimal neuroprotective activity at 100 nM, this concentration was used in the following mechanistic studies. In summary, these data provided the first line of evidence for an estrogenic agonist profile of **2** action in neurons consistent with 17β-estradiol and **1**.[16]

Mechanistically, the characterization of signal transduction pathways activated by estrogen has led to the identification of proteins that are critical mediators of estrogen activity in neurons. First, estrogen activation of extracellular signal-regulated kinase (ERK) leads to activation of the transcription factor cyclic AMP response element-binding protein, CREB, which results in increased transcription of multiple neuroprotective genes such as Bcl-2 family anti-apoptotic genes[47] and neurotrophic genes such as spinophilin.[48] In parallel, through a unified upstream mechanism, estrogen binding to ER and subsequent interaction with the phosphatidylinositide-3′-OH kinase (PI3′K) activate the protein kinase B (also known as Akt), which phosphorylates the Bcl-2 family pre-apoptotic member BAD, thereby suppressing apoptosis and promoting neuronal survival.[49−52] Our previous analyses demonstrated that **1** was effective in promoting both ERK and Akt phosphorylation in hippocampal neurons.[16] In this experiment, we sought to determine whether **2** would activate these same signaling mechanisms. Rat hippocampal neurons grown for 7 DIV were B27 supplement-deprived for 45 min prior to incubation with vehicle alone, 17β-estradiol (10 nM), or **2** (100 nM) for 30 min prior to harvesting of proteins for detection of phosphorylated ERK and Akt expression by Western immunoblotting analyses. Total ERK and Akt expression levels in the same protein samples were detected and used as loading controls. Results of these analyses indicated that exposure of neurons to **2** rapidly induced a significant increase in phosphorylation of both ERK2 and Akt (Figure 7, 46.3 ± 14.7% and 139.1 ± 33.4% increase compared to vehicle alone treated control cultures, respectively, $^*P < 0.05$), with efficacy slightly lower than but not significantly different from that induced by 17β-estradiol (Figure 7, 38.0 ± 7.7% and 88.0 ± 27.2% increase compared to vehicle alone-treated control cultures, respectively, $^*P < 0.05$).

Estrogen upregulation of Bcl-2 family anti-apoptotic proteins Bcl-2 and Bcl-X_L has been proposed as one critical component underlying estrogen promotion of neuronal survival.[47,49,53] Upregulation of both Bcl-2 and Bcl-X_L expression by **1** was previously observed as well.[16] Accordingly, we evaluated whether **2** regulated these proteins in rat primary hippocampal neurons. Neurons grown for 7 DIV were treated with vehicle alone, 17β-estradiol (10 nM) or **2** (100 nM), for 48 h followed by Western immunoblotting analyses. Results of these analyses indicated that **2** induced a significant increase in both Bcl-2 and Bcl-X_L expression in neurons (Figure 8, 23.4 ± 6.8% and 58.0 ± 22.2% increase compared to vehicle alone treated control cultures, respectively, $^*P < 0.05$), with efficacy comparable to

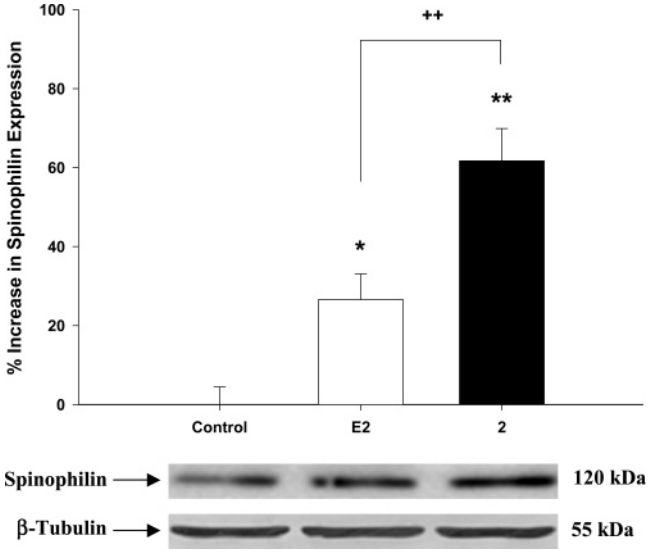

Figure 9. Compound **2** upregulated the dendritic spine protein, spinophilin expression in rat primary hippocampal neurons. Neurons grown for 7 DIV were treated with vehicle alone, E2 (10 nM), or **2** (100 nM) for 48 h followed by Western immunoblotting analyses on spinophilin expression in the whole cell lysate preparation of neurons. β-tubulin was used as an internal loading control protein. Results are presented as percent increase in spinophilin expression compared to vehicle alone treated control cultures and expressed as mean ± SEM, $n = 4$, $^{*}P < 0.05$, $^{**}P < 0.01$, and $^{++}P < 0.01$. E2: 17β-estradiol.

17β-estradiol (Figure 8, 20.7 ± 1.8% and 46.6 ± 11.6% increase compared to vehicle alone-treated control cultures, respectively, $^{*}P < 0.05$).

In addition to regulating Bcl-2 family anti-apoptotic proteins, estrogen activation of CREB leads to increased expression of spinophilin, a protein that is enriched in the heads of neuronal dendritic spines in hippocampal neurons and which is predictive of estrogen-inducible promotion of neuronal morphogenesis and synaptoplasticity.[48] Compound **1** was found to be comparably effective to 17β-estradiol in upregulating spinophilin expression in primary neurons.[16] Based on these earlier findings, we evaluated the impact of **2** on the expression level of spinophilin, as an indicator of its neurotrophic potential, in comparison with 17β-estradiol. Data shown in Figure 9 indicated that exposure of hippocampal neurons to **2** (100 nM) for 48 h induced a significant increase in spinophilin expression. (Figure 9, 61.7 ± 8.2% increase compared to vehicle alone-treated control cultures, $^{**}P < 0.01$). Under the same experimental conditions, 17β-estradiol (10 nM) induced a moderate increase (Figure 9, 26.6 ± 6.5% increase compared to vehicle alone-treated control cultures, $^{*}P < 0.05$), which was significantly less than that induced by **2** ($^{++}P < 0.01$). The present finding is in agreement with our earlier study that showed a similar trend in the difference in magnitude of change in spinophilin expression between 17β-estradiol- and **1**-treated neurons.[16] These data are promising in that they suggest that **2** and its structural analogs, a distinct category of ER ligands from the nuclear ER full agonist as represented by 17β-estradiol, have a greater potential in activating mechanisms of neuronal synaptoplasticity and associated memory function.

Taken together, results of mechanistic analyses provide the second line of evidence for the estrogenic activity of **2** in neurons.

Conclusion

A rationally designed novel mimic of **1**, **2**, with a hybrid structure of 17β-estradiol and vitamin E, was synthesized. Investigation of **2** induction of neuronal responses provides two lines of evidence indicating an estrogenic agonist profile of **2** action in primary hippocampal neurons. First, **2** was found to be a potent neuroprotectant as evidenced by its promotion of both neuronal membrane integrity and metabolic viability against neurodegenerative insult in neurons. Second, **2** effectively activated signaling cascades and increased expression of proteins consistent with estrogenic agonist function in neurons and required for estrogen promotion of neuronal defense and synaptogenesis. These data indicate that our previous discovery of the estrogenic agonist activity of the nuclear ER full antagonist, **1**, in primary neurons,[16] is not an exclusive feature of **1** alone and can be achieved through structural analogs that may have greater BBB penetration potential. Moreover, as proposed for **1**,[16] **2** is likely acting through a membrane-associated ER leading to induction of the downstream singling cascades and neuronal agonistic responses as presented hereinbefore. However, at this time it cannot be ruled out for potential non-ER-mediated sites of action for **2** and similar future compounds which include a phenolic ring as reported by Simpkins and colleagues.[54] Collectively, results of these analyses provide in vitro proof of principle that development of brain-selective SERMs could provide a safe and efficacious therapeutic alternative to existing hormone therapies to promote neurological function and health through the postmenopausal years. In vivo analyses to determine the BBB penetration and impact on the CNS and periphery of **2** are currently underway.

Experimental Section

Chemistry. Melting points were determined on a MEL-TEMP II capillary melting point apparatus and are uncorrected. NMR (^{1}H, ^{13}C, gHSQC, gHMBC, gCOSY, and ROESY) spectra were obtained using a Bruker Avance DPX-300 MHz or a Varian Unity Inova 500 MHz NMR spectrometer. Chemical shifts are reported in parts per million (ppm) with reference to internal solvent. HRMS were recorded on a Waters Autospec Ultima mass spectrometer and were performed at the University of Michigan, Ann Arbor, MI. Elemental analysis was done by Atlantic Microlab Inc., Norcross, GA. Analytical thin-layer chromatography (TLC) was carried out using EMD silica gel 60 F_{254} TLC plates. Flash column chromatography was done on silica gel 60 (230−400 mesh) or on a CombiFlash Companion system using Isco prepacked silica gel columns. Reagents were obtained from Aldrich Chemical Co. and used as received unless otherwise noted.

(6*R*,10*R*)-6,10,14-Trimethylpentadecan-2-one (5).[41] A stirred solution of phytol (**4**, 12.9 g, 440 mmol) in MeOH (25 mL) and CH_2Cl_2 (110 mL) at −78 °C was bubbled with a stream of ozone until a blue color persisted in the solution. Afterward, nitrogen was bubbled through the solution until the blue color disappeared. Dimethyl sulfide (25 mL) was added and the mixture was allowed to stir at room temperature for 2.5 h. The solvent was removed under reduced pressure and the residue was partitioned between H_2O (100 mL) and benzene (300 mL). The organic phase was separated, washed with brine (150 mL), dried (Na_2SO_4), and concentrated under reduced pressure. Flash column chromatography on silica gel (300 g) using 10% EtOAc in hexane gave 6.49 g of pure **5** and 4.12 g of less pure product. Further purification of the less pure product on a silica gel column (120 g) using 5 → 10% EtOAc in hexane afforded another 2.41 g of pure **5**, for a combined yield of 76%, as an oil. ^{1}H NMR (300 MHz, $CDCl_3$) δ 0.83−0.88 (m, 12H), 1.03−1.64 (m, 19H), 2.13 (s, 3H), 2.40 (t, $J = 7.4$ Hz, 2H); ^{13}C NMR (75 MHz, $CDCl_3$) δ 19.5, 19.6, 21.3, 22.5, 22.6, 24.1, 24.7, 27.9, 29.6, 32.6, 32.7, 36.4, 37.1, 37.2, 37.3, 39.3, 44.0, 208.8.

(4*R*,8*R*)-1-Acetoxy-4,8,12-trimethyltridecane (6). To a stirred solution of **5** (7.00 g, 26.1 mmol) and bis(trimethylsilyl)peroxide (4.70 g, 26.3 mmol, Gelest Inc., Morrisville, PA) in anhydrous CH_2Cl_2 (260 mL) at 0 °C under argon was slowly added $SnCl_4$ (6.90

g, 26.5 mmol). After addition, the solution was stirred at 0 °C for 15 min, warmed to room temperature, and stirred for 1 h. An additional amount of bis(trimethylsilyl)peroxide (4.70 g, 26.3 mmol) was added and the mixture was stirred for 3 h. The reaction mixture was poured into a 10% $Na_2S_2O_3$ solution (260 mL) and extracted with ether (350 mL and 2 × 250 mL). The combined organic extracts were washed with a saturated $NaHCO_3$ solution (200 mL), dried (Na_2SO_4), and concentrated under reduced pressure. Flash column chromatography on silica gel (330 g) using 5% EtOAc in hexane gave 3.18 g of pure **6** and 2.31 g of less pure product. Further purification of the less pure product on a silica gel column (120 g) using 5% EtOAc in hexane afforded another 1.43 g of pure **6**, for a combined yield of 62%, as an oil. ^{1}H NMR (300 MHz, $CDCl_3$) δ 0.83−0.88 (m, 12H), 1.02−1.71 (m, 19H), 2.05 (s, 3H), 4.04 (t, J = 6.8 Hz, 2H); ^{13}C NMR (75 MHz, $CDCl_3$) δ 19.5, 19.7, 20.9, 22.5, 22.6, 24.4, 24.7, 26.1, 27.9, 32.4, 32.7, 33.0, 37.1, 37.2, 37.3, 39.3, 64.8, 170.9; HRMS (ESI) calcd for $C_{18}H_{36}O_2$ [M + Na]$^+$, 307.2613; found, 307.2613.

(4*R*,8*R*)-4,8,12-Trimethyltridecanol (7). To a stirred solution of **6** (4.10 g, 14.4 mmol) in MeOH (90 mL) was added *p*-TsOH (110 mg, 0.58 mmol) and the reaction mixture was refluxed for 6 h. After cooling to room temperature, the solvent was removed under reduced pressure. The residue was dissolved in CH_2Cl_2 (50 mL) and the CH_2Cl_2 solution was washed with a saturated $NaHCO_3$ solution (50 mL). The aqueous layer was extracted with CH_2Cl_2 (2 × 50 mL). The combined CH_2Cl_2 extracts were dried (Na_2SO_4). Removal of the solvent under reduced pressure afforded crude **7** (3.50 g, 100%) as an oil, which was used in the next step without further purification. ^{1}H NMR (300 MHz, $CDCl_3$) δ 0.83−0.88 (m, 12H), 1.01−1.66 (m, 19H), 3.63 (m, 2H); ^{13}C NMR (75 MHz, $CDCl_3$) δ 19.6, 19.7, 22.5, 22.6, 24.4, 24.7, 27.9, 30.3, 32.6, 32.7, 32.9, 37.2, 37.3, 37.4, 39.3, 63.1.

(4*R*,8*R*)-1-Iodo-4,8,12-trimethyltridecane (8). To a stirred solution of triphenylphosphine (1.30 g, 4.96 mmol) in anhydrous CH_2Cl_2 (17 mL) at room temperature under argon was added imidazole (0.35 g, 5.13 mmol) followed by iodine (1.25 g, 4.94 mmol). After stirring for 15 min, a solution of **7** (1.00 g, 4.12 mmol) in anhydrous CH_2Cl_2 (6 mL) was added to the mixture and the stirring was continued for another 1.75 h. The mixture was filtered and the solid was washed with CH_2Cl_2. The filtrate was concentrated under reduced pressure. Flash column chromatography on silica gel (120 g) using hexane afforded **8** (1.23 g, 85%) as an oil. ^{1}H NMR (300 MHz, $CDCl_3$) δ 0.84−0.88 (m, 12H), 1.02−1.89 (m, 19H), 3.17 (dt, J = 7.0, 1.5 Hz, 2H); ^{13}C NMR (75 MHz, $CDCl_3$) δ 7.3, 19.7, 19.8, 22.6, 22.7, 24.4, 24.8, 28.0, 31.3, 32.1, 32.8, 37.2, 37.3, 37.4, 38.0, 39.4; HRMS (EI) calcd for $C_{16}H_{33}I$ [M$^+$], 352.1627; found, 352.1634.

6-Oxo-3,17β-estradiol Diacetate (10).[43] To a stirred mixture of CrO_3 (37.4 g, 375 mmol) in anhydrous CH_2Cl_2 (235 mL) at −20 °C under nitrogen was added 3,5-dimethylpyrazole (35.6 g, 375 mmol). After stirring for 20 min, 3,17β-estradiol diacetate (**9**, 5.34 g, 15.0 mmol) was added and the reaction mixture was stirred at −20 to −15 °C for 5 h. Thereafter, 5 N NaOH (150 mL) was added and the mixture was stirred at −10 °C for 45 min. The mixture was diluted with H_2O (200 mL) and the CH_2Cl_2 phase was separated. The aqueous phase was extracted with CH_2Cl_2 (3 × 200 mL). The combined CH_2Cl_2 extracts were washed with 1 N HCl (2 × 100 mL) and brine (200 mL), dried (Na_2SO_4), and concentrated under reduced pressure. Flash column chromatography on silica gel (200 g) using 10 → 30% EtOAc in hexane afforded **10** (2.43 g, 44%) as a white foam. ^{1}H NMR (300 MHz, $CDCl_3$) δ 0.84 (s, 3H), 1.35−1.80 (m, 6H), 1.95−2.05 (m, 2H), 2.07 (s, 3H), 2.20−2.30 (m, 2H), 2.31 (s, 3H), 3.26−3.38 (m, 1H), 2.51−2.61 (m, 1H), 2.76 (dd, J = 16.8, 3.3 Hz, 1H), 4.72 (dd, J = 9.0, 7.8 Hz, 1H), 7.26 (dd, J = 8.7, 2.7 Hz, 1H), 7.44 (d, J = 8.7 Hz, 1H), 7.75 (d, J = 2.7 Hz, 1H); ^{13}C NMR (75 MHz, $CDCl_3$) δ 11.5, 20.6, 20.7, 22.6, 24.9, 27.1, 36.0, 39.1, 42.3, 43.3, 49.2, 81.7, 119.5, 126.4, 126.6, 133.2, 143.8, 149.0, 168.8, 170.4, 196.0.

6-Oxo-3,17β-estradiol (11). To a stirred solution of **10** (2.40 g, 6.50 mmol) in MeOH (100 mL) and THF (50 mL) at room temperature was added 2 N KOH (20 mL). After stirring for 4 h, the reaction mixture was concentrated under reduced pressure. The residue was taken up in 1 N HCl (50 mL) and extracted with EtOAc (3 × 50 mL). The combined EtOAc extracts were dried (Na_2SO_4). Removal of the solvent under reduced pressure afforded crude **11** (1.95 g, 100%) as a white foam, which was used in the next step without further purification. ^{1}H NMR (300 MHz, DMSO-d_6) δ 0.66 (s, 3H), 1.15−1.62 (m, 8H), 1.70−1.95 (m, 2H), 2.20−2.50 (m, 3H), 3.48−3.60 (m, 1H), 4.48 (d, J = 4.8 Hz, 1H), 6.99 (dd, J = 8.5, 2.8 Hz, 1H), 7.27 (d, J = 2.8 Hz, 1H), 7.31 (d, J = 8.5 Hz, 1H), 9.59 (s, 1H); ^{13}C NMR (75 MHz, DMSO-d_6) δ 11.0, 22.4, 25.1, 28.3, 29.7, 36.1, 42.1, 42.5, 43.4, 49.1, 79.8, 111.7, 121.2, 126.7, 132.9, 137.8, 155.6, 197.1.

3,17β-Bis(2-tetrahydropyranyloxy)estra-1,3,5(10)-triene-6-one (12).[44] To a stirred suspension of crude **11** (1.95 g, 6.50 mmol) in anhydrous CH_2Cl_2 (65 mL) at room temperature under nitrogen was added dihydropyran (5.89 mL, 65.0 mmol) and pyridinium *p*-toluenesulfonate (33 mg). The mixture was refluxed for 4 h, cooled to room temperature, and diluted with CH_2Cl_2 (100 mL). The solution was washed with brine (3 × 30 mL), dried (Na_2SO_4), and concentrated under reduced pressure. Flash column chromatography on silica gel (40 g Isco prepacked column) using 0 → 20% EtOAc in hexane afforded **12** (2.88 g, 98%) as a white foam. ^{1}H NMR (300 MHz, $CDCl_3$) δ 0.81, 0.82 (2s, 3H), 1.20−2.28 (m, 22H), 2.30−2.50 (m, 2H), 2.73 (dd, J = 16.8, 3.3 Hz, 1H), 3.45−3.65 (m, 2H), 3.73 (q, J = 8.4 Hz, 1H), 3.80−4.00 (m, 2H), 4.60−4.70 (m, 1H), 5.46−5.52 (m, 1H), 7.23 (dd, J = 8.5, 2.7 Hz, 1H), 7.33, 7.35 (2d, J = 8.5 Hz, 1H), 7.71, 7.72 (2d, J = 2.7 Hz, 1H); HRMS (ESI) calcd for $C_{28}H_{38}O_5$ [M + Na]$^+$, 477.2617; found, 477.2611.

3,17β-Bis(2-tetrahydropyranyloxy)-7α-(4*R*,8*R*,12-trimethyltridecyl)estra-1,3,5(10)-triene-6-one (13). To a stirred solution of **12** (0.46 g, 1.01 mmol) in DME (5 mL) at room temperature under nitrogen was added a 1 M solution of potassium *t*-butoxide (1.11 mL, 1.11 mmol) in THF. After stirring for 10 min, a 1 M solution of triethyl-borane (1.26 mL, 1.26 mmol) in THF was added and stirring was continued for 1 h at room temperature. A solution of **8** (444 mg, 1.26 mmol) in DME (2 mL) was then added to the resulting enolate. After stirring for 40 min, an additional equivalent of potassium *t*-butoxide solution was added and the mixture was stirred for another 16 h. The reaction was quenched with H_2O (20 mL) and extracted with EtOAc (4 × 50 mL). The combined EtOAc extracts were dried (Na_2SO_4) and concentrated under reduced pressure. Flash column chromatography on silica gel (40 g Isco prepacked column) using of 0 → 20% EtOAc in hexane afforded **13** (232 mg, 34%) as an oil. ^{1}H NMR (300 MHz, $CDCl_3$) δ 0.75−0.91 (m, 15H), 0.95−1.76 (m, 36H), 1.78−2.18 (m, 6H), 2.28−2.50 (m, 2H), 2.52−2.68 (m, 1H), 3.45−3.68 (m, 2H), 3.75 (q, J = 8.4 Hz, 1H), 3.85−4.00 (m, 2H), 4.62−4.73 (m, 1H), 5.44−5.52 (m, 1H), 7.20 (dd, J = 8.4, 2.4 Hz, 1H), 7.31, 7.32 (2d, J = 8.4 Hz, 1H), 7.69 (s, 1H); ^{13}C NMR (75 MHz, $CDCl_3$) δ 11.7, 19.0, 19.1, 19.6, 19.8, 19.9, 22.5, 22.6, 22.8, 22.9, 24.1, 24.2, 24.7, 25.0, 25.4, 25.8, 26.9, 27.3, 28.2, 28.9, 30.5, 31.2, 31.3, 32.9, 33.0, 37.2, 37.3, 37.5, 37.6, 37.7, 39.6, 42.5, 42.6, 42.7, 43.0, 43.5, 45.5, 45.6, 48.9, 49.0, 49.1, 62.1, 62.4, 62.5, 62.7, 84.2, 85.6, 96.6, 96.8, 96.9, 99.5, 114.9, 122.4, 122.5, 127.1, 127.2, 132.6, 139.6, 139.8, 155.7, 155.8, 201.0, 201.1; HRMS (ESI) calcd for $C_{44}H_{70}O_5$ [M + Na]$^+$, 701.5121; found, 701.5125.

7α-[(4*R*,8*R*)-4,8,12-Trimethyltridecyl]estra-1,3,5(10)-trien-3,-17β-diol (2). To a stirred solution of **13** (207 mg, 0.30 mmol) in anhydrous CH_2Cl_2 (13 mL) at room temperature under nitrogen was added triethylsilane (3.35 mL, 21.0 mmol). The mixture was cooled to 0 °C and boron trifluoride etherate (11.3 mL, 90.0 mmol) was added dropwise. The yellow solution was warmed to room temperature and stirred for 16 h. The reaction was carefully hydrolyzed with a 10% K_2CO_3 solution (60 mL) and then passed through a plug of silica gel. The filtrate was extracted with CH_2Cl_2 (4 × 50 mL). The combined CH_2Cl_2 extracts were dried (Na_2SO_4) and concentrated under reduced pressure. Flash column chromatography on silica gel (40 g Isco prepacked column) using 0 → 20% EtOAc in hexane afforded **2** (126 mg, 83%) as a white foam. ^{1}H NMR (500 MHz; $CDCl_3$) δ 0.79 (s, 3H), 0.81−0.90 (m,

12H), 1.00−1.58 (m, 26H), 1.58−1.66 (m, 2H), 1.72−1.78 (m, 1H), 1.90 (d, J = 12.5 Hz, 1H), 2.09−2.18 (m, 1H), 2.26−2.35 (m, 2H), 2.72 (d, J = 16.9 Hz, 1H), 2.86 (dd, J = 16.9, 4.8 Hz, 1H), 3.76 (t, J = 8.5 Hz, 1H), 5.24 (br s, 1H), 6.56 (s, 1H), 6.63 (d, J = 8.5 Hz, 1H), 7.14 (d, J = 8.5 Hz, 1H); ^{13}C NMR (125 MHz; $CDCl_3$) δ 11.3, 19.9, 22.8, 22.9, 24.7, 25.0, 25.7, 26.0, 27.4, 28.2, 30.7, 33.0, 33.3, 34.7, 37.0, 37.4, 37.6, 37.7, 38.2, 39.5, 42.1, 43.6, 46.6, 82.3, 113.0, 116.3, 127.2, 132.0, 137.3, 153.6; HRMS (ESI) calcd for $C_{34}H_{56}O_2[M + Na]^+$, 519.4178; found, 519.4182. Anal. ($C_{34}H_{56}O_2 \cdot 0.25\ H_2O$) C, H.

Computer Modeling. All calculations were performed on a SGI Octane graphical workstation equipped with the IRIX 6.5 operating system (Silicon Graphics Inc., Mountain View, CA), using a comprehensive suite of molecular modeling and simulation program, InsightII 2000 (Accelrys Inc., San Diego, CA), and an automated ligand docking program, GOLD 3.0 (Genetic Optimization for Ligand Docking), distributed by CCDC (Cambridge Crystallographic Data Center). InsightII provides a 3D molecular graphics interface integrated with sets of modeling tools for building, visualizing, and analyzing molecular structures. GOLD provides a docking tool for predicting the binding modes of small molecules into protein binding sites, and it has been highly regarded for its accuracy and reliability.[55,56] Using a genetic algorithm (GA), GOLD explores a full range of conformational flexibility of the ligand and partial flexibility of the protein. In the present study, compounds **1** and **2** were first built and energy minimized with the Build module in InsightII, followed by docking analyses using GOLD. The 3D structural coordinate data of hERα LBD with a defined ligand docking site, which was used as the target protein in the docking runs, were derived from a template crystal structure available in the Protein Data Bank (PDB entry: 1HJ1).[18] 1HJ1 contains the 3D coordinate data, resolved by X-ray diffraction, of rat ERβ LBD complexed with **3**, a structural analog of **1**.[18] Briefly, the 3D structures of the LBDs of hERα (PDB entry: 1ERR)[22] and rERβ in complex with **3**,[18] were superimposed based upon the α-atoms in the backbone chains of two receptors. rERβ was removed from the complex and the remaining hERα and **3** were associated as a new assembly. Following removal of water molecules included in hERα and hydrogenation at a pH of 7.0, the resultant complex was energetically optimized with the Discover module in InsightII under a consistent-valence forcefield. Then, based on the binding position of **3** in hERα, a ligand docking site that includes all atoms within a probe radius of 15 Å centered at the coordinate of a carbon atom located at the middle of the 7α-side chain in **3**, was defined. Fifty GA runs were carried out with standard default settings, a population size of 100, a maximum of 100 000 operations, and a mutation and crossover of 95. GOLD offers a choice of fitness functions: GoldScore and ChemScore. GoldScore, which has been optimized for the prediction of ligand binding positions, was used in the present study. GoldScore is made up of four components and quantitated by the following equation: $f = S_{hb\_ext} + S_{vdw\_ext} + S_{hb\_int} + S_{vdw\_int}$, where S_{hb_ext} is the protein−ligand hydrogen bonding score and S_{hb_int} is the internal hydrogen bonding of the ligand. Usually, the best result is obtained by letting the internal hydrogen bonding tend to zero. S_{vdw_ext} and S_{vdw_int} are the scores arising from weak van der Waals forces. S_{vdw_ext} is multiplied by a factor of 1.375 when the total fitness score is computed, which is an empirical correction to encourage protein−ligand hydrophobic contact. Three top-ranked solutions were collected and analyzed in the context of hERα in InsightII. Taking into account the importance of the hydrogen bonding interactions between the polar residues, glu353 and his524, along the ER binding site, and the hydroxyl groups attached to the core structural moiety in ER ligands for a strong binding, as revealed in our previous analyses,[21] solutions with the highest S_{vdw_ext} were specified as the final bound conformations for both **1** and **2**. In detail, the bound conformation for **1** has a fitness score of 79.79, computed from individual scores of 6.95, 61.48, 0.00, and −11.69 for each of four components, S_{hb_ext}, S_{vdw_ext}, S_{hb_int}, and S_{vdw_int}, included in the fitness function, GoldScore. Compound **2** binds to hERα in an analogous mode to **1**, with a fitness score of 74.73, computed from individual scores of, 6.16, 62.67, 0.00, and −17.60 for S_{hb_ext}, S_{vdw_ext}, S_{hb_int}, and S_{vdw_int}, respectively.

ER Competitive Binding. The ER binding affinity and selectivity of **2** and control compounds were determined by a fluorescent polarization competitive binding assay using purified baculovirus-expressed human ERα or ERβ and a fluorescent estrogen ligand EL Red (Invitrogen, Calsbad, CA). Test compounds were serially diluted to a 2× concentration in assay buffer (20 μM to 200 pM). A total of 40 μL of assay buffer mixed with 2× test compounds was added to a 384-well nonbinding surface black microplate (Corning Life Sciences, Acton, MA), followed by the addition of 40 μL of preincubated 2× complex of ERα (30 nM) or ERβ (60 nM) and EL Red (2 nM) for a final volume of 80 μL. Negative controls containing ER and EL Red (equivalent to 0% inhibition) and positive controls containing only free EL Red (equivalent to 100% inhibition) were included. After a 6-hour incubation period at room temperature, the polarization values were measured using a GENios Pro microplate reader (Tecan, Mannedorf/Zurich, Switzerland) at excitation/emission 535/590 nm and plotted against the logarithm of the test compound concentration. The ER/EL Red complex has a high polarization value yielded from a slow stumbling due to its large size. If the test compound competes for estrogen binding, it displaces the EL Red from the ER/EL Red complex and causes a reduced polarization value. A noncompetitor does not displace the EL Red from the ER/EL Red complex, and the polarization value remains high. IC_{50} value, the concentration of the test compound that displaces half of the EL Red from ER, was determined from the plot using a nonlinear least-squares analysis using GraphPad Prism, version 4.03 (GraphPad Software, San Diego, CA).

Rat Primary Hippocampal Neuronal Cultures. The use of animals was approved by the Institutional Animal Care and Use Committee (IACUC) at the University of Southern California. Primary cultures of rat hippocampal neurons were prepared according to the method described previously.[57] Briefly, hippocampi were dissected from the brains of fetuses derived from embryonic day 18 Sprague−Dawley rats (Harlan Sprague Dawley, Indianapolis, IN) treated with 0.02% trypsin in Hank's balanced salt solution (137 mM NaCl, 5.4 mM KCl, 0.4 mM KH_2PO_4, 0.34 mM $Na_2HPO_4 \cdot 7H_2O$, 10.0 mM glucose, and 10.0 mM HEPES) at 37 °C for 5 min and dissociated by repeated passage through a series of fire-polished constricted Pasteur pipettes. Approximately 10^6 cells/mL were seeded onto poly-D-lysine-coated solid black and clear bottom 96-well culture plates for neuroprotection and 60 mm petri dishes for Western immunoblotting analyses. Cells were grown in phenol-red free Neurobasal medium (NBM, Invitrogen), supplemented with B27, 5 U/mL penicillin, 5 μg/mL streptomycin, 0.5 mM glutamine, and 25 μM glutamate at 37 °C in 10% CO_2 for the first 3 d and NBM without glutamate afterward. Cultures grown in serum-free NBM yield approximately 99.5% neurons and 0.5% glial cells.

Glutamate Exposure. Primary hippocampal neurons grown on solid black and clear bottom 96-well culture plates for 7 d in vitro (DIV) were pretreated with vehicle alone or **2** at serially diluted concentrations (1, 10, 100, and 1000 nM) for 48 h, followed by exposure to 200 μM glutamate at room temperature for 5 min in HEPES-buffered saline solution (HBS, containing 100 mM NaCl, 2.0 mM KCl, 2.5 mM $CaCl_2$, 1.0 mM $MgSO_4$, 1.0 mM NaH_2PO_4, 4.2 mM $NaHCO_3$, 10.0 mM glucose, and 12.5 mM HEPES). Immediately following glutamate exposure, cultures were washed once with HBS and replaced with fresh NBM containing vehicle alone or **2**. Cultures were returned to the culture incubator and allowed to incubate for an additional 24 h prior to neuronal viability measurements on the following day.

Neuronal Viability. LDH Release Measurement: LDH is a stable cytoplasmic enzyme present in all cells including neurons. It is rapidly released into the cell culture supernatant when the cell plasma membrane is damaged. Thus, the LDH level in the culture medium is a reliable biochemical index for neuronal plasma membrane damage. In this study, LDH released from the cytosol

of damaged neurons into the culture medium following glutamate exposure was measured using a CytoTox-ONE homogeneous membrane integrity assay (Promega Corp., Madison, WI), which determines the LDH activity in the culture medium to enzymaticly convert the lactate and NAD^+ to pyruvate and NADH. In the enzymatic reaction, the substrate resazurin is reduced to fluorescent resorufin in the presence of diaphorase, thereby allowing a fluorometric detection and the signal detected is proportional to the amount of LDH. Briefly, 40 μL of culture medium from each well of the culture plate was transferred to a 384-well nonbinding surface black microplate (Corning Life Sciences) and 40 μL of the assay reagent was added to incubate at room temperature for 10 min. The fluorescent signal was measured on a SpectraMax microplate spectrofluorometer (Molecular Devices, Sunnyvale, CA) at excitation/emission 560/590 nm.

Calcein AM Staining: Calcein AM (Molecular Probes, Eugene, OR) is a fluorogenic esterase substrate that enters live cells through permeability and is enzymatically hydrolyzed to form the polyanionic dye calcein, which is well-retained within live cells due to the intact plasma membranes and produces an intense uniform green fluorescence at 530 nm. Thus, calcein AM serves as a reliable indicator of intact and metabolically viable cells in the cultures. Following glutamate exposure, after the culture medium was taken out for LDH release measurement, cultures were rinsed with warm PBS once and incubated with 1 μM calcein AM in PBS at room temperature for 30 min. The fluorescent signal was measured on a SpectraMax microplate spectrofluorometer (Molecular Devices) at excitation/emission 485/530 nm.

Western Immunoblotting. Primary hippocampal neurons grown on poly-D-lysine-coated culture dishes for 7 DIV were treated with vehicle alone or test compounds for 30 min (for analyses on pERK2/ERK2 and pAkt/Akt expression) or 48 h (for analyses on Bcl-2, Bcl-X_L, spinophilin, and β-tubulin expression). Cultures were washed with cold PBS once and scraped off the dish in 1 mL PBS. Cells were then centrifuged at 5000 rpm for 5 min, and the pellets were dissolved in the RIPA lysis buffer (PBS, 1% Triton, 0.2% SDS, and protease and phosphatase inhibitor cocktail set I (Cal-BioChem, San Diego, CA)) and suspended by passage through a 200 μL pipet tip. Following incubation at 4 °C for 45 min, the samples were centrifuged at 12 000 rpm for 10 min, and the supernatants were collected as the whole cell protein extracts. Protein concentration was determined by the Bicinchoninic Acid method. A total of 20 μg of protein samples were diluted in 15 μL 2× SDS containing sample buffer and the final volume was made 30 μL with water. After denaturation on a hot plate at 95−100 °C for 5 min, 20 μL of the mixture were loaded per lane on 10% SDS-polyacrylamide mini-gels followed by electrophoresis at 90V. A high-range Precision Protein Standard (Bio-Rad Laboratories, Hercules, CA) was used to determine the protein size. The proteins were then electrotransferred to polyvinylidene difluoride membranes (Millipore Corp., Bedford, MA) from the gels. Nonspecific binding sites were blocked with 5% nonfat dry milk in PBS containing 0.05% Tween-20 (PBS-Tween). Membranes were incubated with primary antibodies directed against phospho-ERK1/2 ($pTpY^{185/187}$, 1:1000 dilution, polyclonal, Biosource International, Camarillo, CA), phospho-Akt (pS^{473} 1:2000 dilution, monoclonal, Cell Signaling Technology, Beverly, MA), Bcl-2 (1:250 dilution, monoclonal, Zymed Laboratories, San Francisco, CA), Bcl-X_L (1:500 dilution, monoclonal, Zymed Laboratories), or spinophilin (1:500 dilution, polyclonal, Upstate, Charlottesville, VA) in PBS-Tween at 4 °C overnight and then incubated with the horseradish peroxidase (HRP)-conjugated secondary antibodies (Vector Laboratories, Burlingame, CA) at room temperature for 2 h. After scanning, membranes were stripped and reprobed with the primary antibodies against ERK2 (1:5000 dilution, polyclonal, Santa Cruz Biotechnology), Akt (1:1,000 dilution, polyclonal, Cell Signaling Technology), or β-tubulin (1:5,000 dilution, polyclonal, Abcam, Cambridge, MA) at room temperature for 2 h, followed by incubation with the HRP-conjugated secondary antibodies (Vector Laboratories) at room temperature for 2 h. Immunoreactive bands were detected by a 3′,3′,5′,5′-tetramethyl-benzidine (TMB) peroxidase substrate kit (Vector Laboratories). Relative intensities of the immunoreactive bands were quantified by optical density analysis using an image digitizing software, Un-Scan-It version 5.1 (Silk Scientific, Orem, UT).

Statistical Analyses. Data are presented as group means ± SEM. Statistically significant differences were determined by a one-way analysis of variance (ANOVA) followed by a Student−Newman−Keuls post hoc analysis.

Acknowledgment. This work was supported by grants from National Institute of Aging (P01 AG14751-10, Project 2), the Kenneth T. and Eileen L. Norris Foundation, L. K. Whittier Foundation, Stanley Family Trust, and the NIMH Chemical Synthesis and Drug Supply Program to R.D.B. The authors also wish to thank Dr. Anantha Reddy for helpful discussions regarding the steroid side chain synthesis and Dr. Jason Burgess for assistance with NMR spectroscopy.

Supporting Information Available: NMR spectra (^1H, ^{13}C, gHSQC, gHMBC, gCOSY, and ROESY), HRMS, HPLC, and elemental analysis of **2**. This material is available free of charge via the Internet at http://pubs.acs.org.

References

(1) Fillit, H. M. The pharmacoeconomics of Alzheimer's disease. *Am. J. Manage. Care* **2000**, *6*, S1139−S1144.
(2) Brookmeyer, R.; Gray, S.; Kawas, C. Projections of Alzheimer's disease in the United States and the public health impact of delaying disease onset. *Am. J. Public Health* **1998**, *88*, 1337−1342.
(3) Gao, S.; Hendrie, H. C.; Hall, K. S.; Hui, S. The relationship between age, sex, and the incidence of dementia and Alzheimer disease: A meta-analysis. *Arch. Gen. Psychiatry* **1998**, *55*, 809−815.
(4) Zandi, P. P.; Carlson, M. C.; Plassman, B. L.; Welsh-Bohmer, K. A.; Mayer, L. S.; Steffens, D. C.; Breitner, J. C. Hormone replacement therapy and incidence of Alzheimer disease in older women: The Cache County Study. *JAMA, J. Am. Med. Assoc.* **2002**, *288*, 2123−2129.
(5) Neurgaren, B. L.; Kraines, R. J. Menopausal symptoms in women of various ages. *Psychosom. Med.* **1965**, *27*, 266−273.
(6) Sherwin, B. B., Impact of changing hormonal mileu on psychological functioning. In *Treatment of the postmenopausal woman: Basic and clinical aspects*. Lobo, R. A., Ed.; Lippincott Williams and Wilkins: Philadelphia, 1999; pp 179−188.
(7) Brinton, R. D. A women's health issue: Alzheimer's disease and strategies for maintaining cognitive health. *Int. J. Fertil. Women's Med.* **1999**, *44*, 174−185.
(8) Fillit, H. M.; O'Connell, A. W.; Refolo, L. M. Strategies for drug discovery for cognitive aging and Alzheimer's disease. *J. Mol. Neurosci.* **2002**, *19*, 1−3.
(9) Henderson, V. W. Estrogen replacement therapy for the prevention and treatment of Alzheimer's disease. *CNS Drugs* **1997**, *8*, 343−351.
(10) Zhao, L.; O'Neill, K.; Brinton, R. D. Selective estrogen receptor modulators (SERMs) for the brain: Current status and remaining challenges for developing NeuroSERMs. *Brain Res. Rev.* **2005**, *49*, 472−493.
(11) Brinton, R. D. Estrogen therapy for prevention of Alzheimer's disease not for rehabilitation following onset of disease: the healthy cell bias of estrogen action. In *Synaptic Plasticity: Basic Mechanisms to Clinical Applications*. Baudry, M., Bi, R., Schreiber, S. S., Ed.; Taylor & Francis Group: New York, 2004; pp 131−157.
(12) Chen, S.; Nilsen, J.; Brinton, R. D. Dose and temporal pattern of estrogen exposure determines neuroprotective outcome in hippocampal neuons: therapeutic implications. *Endocrinology* **2006**, *147*, 5303−5313.
(13) Hammond, C. B. Women's concerns with hormone replacement therapy-compliance issues. *Fertil. Steril.* **1994**, *62*, 157S−160S.
(14) Wassertheil-Smoller, S.; Hendrix, S. L.; Limacher, M.; Heiss, G.; Kooperberg, C.; Baird, A.; Kotchen, T.; Curb, J. D.; Black, H.; Rossouw, J. E.; Aragaki, A.; Safford, M.; Stein, E.; Laowattana, S.; Mysiw, W. J. Effect of estrogen plus progestin on stroke in postmenopausal women: The Women's Health Initiative: A randomized trial. *JAMA, J. Am. Med. Assoc.* **2003**, *289*, 2673−2684.
(15) Manson, J. E.; Hsia, J.; Johnson, K. C.; Rossouw, J. E.; Assaf, A. R.; Lasser, N. L.; Trevisan, M.; Black, H. R.; Heckbert, S. R.; Detrano, R.; Strickland, O. L.; Wong, N. D.; Crouse, J. R.; Stein, E.; Cushman, M. Estrogen plus progestin and the risk of coronary heart disease. *N. Engl. J. Med.* **2003**, *349*, 523−534.

(16) Zhao, L.; O'Neill, K.; Brinton, R. D. Estrogenic agonist activity of ICI 182,780 (Faslodex) in hippocampal neurons: implications for basic science understanding of estrogen signaling and development of estrogen modulators with a dual therapeutic profile. *J. Pharmacol. Exp. Ther.* **2006**, *319*, 1124−1132.
(17) Wakeling, A. E.; Dukes, M.; Bowler, J. A potent specific pure antiestrogen with clinical potential. *Cancer Res.* **1991**, *51*, 3867−3873.
(18) Pike, A. C.; Brzozowski, A. M.; Walton, J.; Hubbard, R. E.; Thorsell, A. G.; Li, Y. L.; Gustafsson, J. A.; Carlquist, M. Structural insights into the mode of action of a pure antiestrogen. *Structure* **2001**, *9*, 145−153.
(19) Howell, A.; Osborne, C. K.; Morris, C.; Wakeling, A. E. ICI 182,-780 (Faslodex): Development of a novel, "pure" antiestrogen. *Cancer* **2000**, *89*, 817−825.
(20) Bross, P. F.; Cohen, M. H.; Williams, G. A.; Pazdur, R. FDA drug approval summaries: fulvestrant. *Oncologist* **2002**, *7*, 477−480.
(21) Zhao, L.; Brinton, R. D. Structure-based virtual screening for plant-based ERβ-selective ligands as potential preventative therapy against age-related neurodegenerative diseases. *J. Med. Chem.* **2005**, *48*, 3463−3466.
(22) Brzozowski, A. M.; Pike, A. C.; Dauter, Z.; Hubbard, R. E.; Bonn, T.; Engstrom, O.; Ohman, L.; Greene, G. L.; Gustafsson, J. A.; Carlquist, M. Molecular basis of agonism and antagonism in the oestrogen receptor. *Nature* **1997**, *389*, 753−758.
(23) Fawell, S. E.; Lees, J. A.; White, R.; Parker, M. G. Characterization and colocalization of steroid binding and dimerization activities in the mouse estrogen receptor. *Cell* **1990**, *60*, 953−962.
(24) Navarro, A.; Gomez, C.; Sanchez-Pino, M. J.; Gonzalez, H.; Bandez, M. J.; Boveris, A. D.; Boveris, A. Vitamin E at high doses improves survival, neurological performance, and brain mitochondrial function in aging male mice. *Am. J. Physiol.* **2005**, *289*, R1392−1399.
(25) Lipinski, C. A.; Dominy, B. W.; Feeney, P. J. Experimental and computational approaches to estimate solubility and permeability in drug discovery and development settings. *Adv. Drug Delivery Rev.* **1997**, *23*, 3−25.
(26) Abbott, N. J.; Ronnback, L.; Hansson, E. Astrocyte-endothelial interactions at the blood-brain barrier. *Nat. Rev. Neurosci.* **2006**, *7*, 41−53.
(27) Habgood, M. D.; Begley, D. J.; Abbott, N. J. Determinants of passive drug entry into the central nervous system. *Cell. Mol. Neurobiol.* **2000**, *20*, 231−253.
(28) Atkinson, F.; Cole, S.; Green, C.; van de Waterbeemd, H. Lipophilicity and other parameters affecting brain penetration. *Curr. Med. Chem.* **2002**, *2*, 229−240.
(29) Iyer, M.; Mishru, R.; Han, Y.; Hopfinger, A. J. Predicting blood-brain barrier partitioning of organic molecules using membrane-interaction QSAR analysis. *Pharm. Res.* **2002**, *19*, 1611−1621.
(30) Ma, X. L.; Chen, C.; Yang, J. Predictive model of blood-brain barrier penetration of organic compounds. *Acta Pharmacol. Sin.* **2005**, *26*, 500−512.
(31) Loscher, W.; Potschka, H. Role of drug efflux transporters in the brain for drug disposition and treatment of brain diseases. *Prog. Neurobiol.* **2005**, *76*, 22−76.
(32) Misra, A.; Ganesh, S.; Shahiwala, A.; Shah, S. P. Drug delivery to the central nervous system: A review. *J. Pharm. Sci.* **2003**, *6*, 252−273.
(33) Bowler, J.; Lilley, T. J.; Pittam, J. D.; Wakeling, A. E. Novel steroidal pure antiestrogens. *Steroids* **1989**, *54*, 71−99.
(34) French, A. N.; Wilson, S. R.; Welch, M. J.; Katzenellenbogen, J. A. A synthesis of 7 alpha-substituted estradiols: Synthesis and biological evaluation of a 7 alpha-pentyl-substituted BODIPY fluorescent conjugate and a fluorine-18-labeled 7 alpha-pentylestradiol analog. *Steroids* **1993**, *58*, 157−169.
(35) Tedesco, R.; Katzenellenbogen, J. A.; Napolitano, E. An expeditious route to 7a-substituted estradiol derivatives. *Tetrahedron Lett.* **1997**, *38*, 7997−8000.
(36) Adamczyk, M.; Johnson, D. D.; Reddy, R. E. A stereoselective synthesis of 7 alpha-(3-carboxypropyl) estradiol from a noncontrolled substance. *Steroids* **1997**, *62*, 771−775.
(37) Skaddan, M. B.; Wust, F. R.; Katzenellenbogen, J. A. Synthesis and binding affinities of novel recontaining 7α-substituted estradiol complexes: Models for breast cancer imaging agents. *J. Org. Chem.* **1999**, *64*, 8108−8121.
(38) Hussey, S. L.; He, E.; Peterson, B. R. Synthesis of chimeric 7α-substituted estradiol derivatives linked to cholesterol and cholesteryl-amine. *Org. Lett.* **2002**, *4*, 415−418.
(39) Blazejewski, J. C.; Wilmshurst, M. P.; Popkin, M. D.; Wakselman, C.; Laurent, G.; Nonclercq, D.; Cleeren, A.; Ma, Y.; Seo, H. S.; Leclercq, G. Synthesis, characterization and biological evaluation of 7α-perfluoroalkylestradiol derivatives. *Bioorg. Med. Chem.* **2003**, *11*, 335−345.
(40) Jiang, X. R.; Sowell, J. W.; Zhu, B. T. Synthesis of 7α-substituted derivatives of 17β-estradiol. *Steroids* **2006**, *71*, 334−342.
(41) Suga, T.; Ohta, S.; Nakai, A.; Munesada, K. Glycinoprenols: novel polyprenols possessing a phytyl residue from the leaves of soybean. *J. Org. Chem.* **1989**, *54*, 3390−3393.
(42) Matsubara, S.; Takai, K.; Nozaki, H. Baeyer−Villiger oxidation with $Me_3SiOOSiMe_3$ under assistance of $SnCl_4$ or $BF_3{\cdot}OEt_2$. *Bull. Chem. Soc. Jpn.* **1983**, *56*, 2029−2032.
(43) Akanni, A. O.; Marples, B. A. Improved preparation of 3,17β-diacetoxyestra-1,3,5(10)-trien-6-one. *Syn. Commun.* **1984**, *14*, 713−715.
(44) Mitra, K.; Marquis, J. C.; Hillier, S. M.; Rye, P. T.; Zayas, B.; Lee, A. S.; Essigmann, J. M.; Croy, R. G. A rationally designed genotoxin that selectively destroys estrogen receptor-positive breast cancer cells. *J. Am. Chem. Soc.* **2002**, *124*, 1862−1863.
(45) Kuiper, G. G.; Carlsson, B.; Grandien, K.; Enmark, E.; Haggblad, J.; Nilsson, S.; Gustafsson, J. A. Comparison of the ligand binding specificity and transcript tissue distribution of estrogen receptors alpha and beta. *Endocrinology* **1997**, *138*, 863−870.
(46) Zhao, L.; Brinton, R. D. Select estrogens within the complex formulation of conjugated equine estrogens (Premarin) are protective against neurodegenerative insults: implications for a composition of estrogen therapy to promote neuronal function and prevent Alzheimer's disease. *BMC Neurosci.* **2006**, *7*, 24.
(47) Wu, T.-W.; Wang, J. M.; Chen, S.; Brinton, R. D. 17β-Estradiol induced Ca2+ influx via L-type calcium channels activates the Src/ERK/cyclic-AMP response element binding protein signal pathway and BCL-2 expresion in rat hippocanpal neurons: A potential initiation mechanism for estrogen-induced neuroprotection. *Neuroscience* **2005**, *135*, 59−72.
(48) Zhao, L.; Chen, S.; Wang, J. M.; Brinton, R. D. 17β-Estradiol induces Ca^{2+} influx, dendritic and nuclear Ca^{2+} rise and subsequent cyclic AMP response element-binding protein activation in hippocampal neurons: a potential initiation mechanism for estrogen neurotrophism. *Neuroscience* **2005**, *132*, 299−311.
(49) Mannella, P.; Brinton, R. D. Estrogen receptor protein interaction with phosphatidylinositol 3-kinase leads to activation of phosphorylated Akt and extracellular signal-regulated kinase 1/2 in the same population of cortical neurons: A unified mechanism of estrogen action. *J. Neurosci.* **2006**, *26*, 9439−9447.
(50) Singh, M. Ovarian hormones elicit phosphorylation of Akt and extracellular-signal regulated kinase in explants of the cerebral cortex. *Endocr. J.* **2001**, *14*, 407−415.
(51) Znamensky, V.; Akama, K. T.; McEwen, B. S.; Milner, T. A. Estrogen levels regulate the subcellular distribution of phosphorylated Akt in hippocampal CA1 dendrites. *J. Neurosci.* **2003**, *23*, 2340−2347.
(52) Datta, S. R.; Dudek, H.; Tao, X.; Masters, S.; Fu, H.; Gotoh, Y.; Greenberg, M. E. Akt phosphorylation of BAD couples survival signals to the cell-intrinsic death machinery. *Cell* **1997**, *91*, 231−241.
(53) Nilsen, J.; Brinton, R. D. Mechanism of estrogen-mediated neuroprotection: regulation of mitochondial calcium and Bcl-2 expression. *Proc. Natl. Acad. Sci. U.S.A.* **2003**, *100*, 2842−2847.
(54) Green, P. S.; Yang, S. H.; Simpkins, J. W. Neuroprotective effects of phenolic A ring oestrogens. *Novartis Found. Symp.* **2000**, *230*, 202−213.
(55) Kellenberger, E.; Rodrigo, J.; Muller, P.; Rognan, D. Comparative evaluation of eight docking tools for docking and virtual screening accuracy. *Proteins* **2004**, *57*, 225−242.
(56) Kontoyianni, M.; McClellan, L. M.; Sokol, G. S. Evaluation of docking performance: Comparative data on docking algorithms. *J. Med. Chem.* **2004**, *47*, 558−565.
(57) Zhao, L.; Wu, T.-W.; Brinton, R. D. Estrogen receptor subtypes alpha and beta contribute to neuroprotection and increased Bcl-2 expression in primary hippocampal neurons. *Brain Res.* **2004**, *1010*, 22−34.

JM070546X